



Synthesis and mesomorphic behavior of novel (bisthiophene)benzene carbazole nematic liquid crystals

Guang Hu, Stuart P. Kitney, Yanfang Liu & Kailong Zhang

To cite this article: Guang Hu, Stuart P. Kitney, Yanfang Liu & Kailong Zhang (2021): Synthesis and mesomorphic behavior of novel (bisthiophene)benzene carbazole nematic liquid crystals, Molecular Crystals and Liquid Crystals, DOI: [10.1080/15421406.2021.1895960](https://doi.org/10.1080/15421406.2021.1895960)

To link to this article: <https://doi.org/10.1080/15421406.2021.1895960>



Published online: 28 Jun 2021.



Submit your article to this journal [↗](#)



Article views: 19



View related articles [↗](#)



View Crossmark data [↗](#)



Synthesis and mesomorphic behavior of novel (bisthiophene)benzene carbazole nematic liquid crystals

Guang Hu^{a,b}, Stuart P. Kitney^c, Yanfang Liu^a, and Kailong Zhang^a

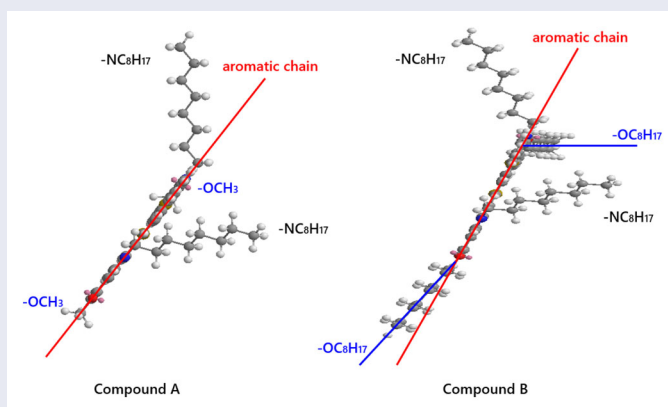
^aKey Laboratory for Palygorskite Science and Applied Technology of Jiangsu Province, National & Local Joint Engineering Research Center for Mineral Salt Deep Utilization, Faculty of Chemical Engineering, Huaiyin Institute of Technology, Huaian, Jiangsu, P. R. China; ^bDepartment of Chemistry, Faculty of Science and Engineering, University of Hull, Cottingham Road, Kingston Upon Hull, UK; ^cPolar OLED, University of Hull, Cottingham Road, Kingston Upon Hull, UK

ABSTRACT

Two structural isomers of highly conjugated (bisthiophene)benzene carbazoles were designed and synthesized to study the effect of the substitution pattern on their liquid crystalline behavior, transition temperatures, energy levels, and band gaps. Unusually, only the isomer A with shorter terminal methyl chains exhibits a liquid crystalline phase, while the isomer B with longer octyl chains does not. It is because longer terminal octyl chains of isomer B strengthen not only the small angle between symmetrical sides of the aromatic backbone, but also the angle between the terminal alkyl chains and the aromatic backbone, thereby leading to a lower length-to-breadth ratio.

KEYWORDS

(bisthiophene)benzene carbazole; 3D molecular configuration; nematic liquid crystalline; Suzuki aryl-aryl cross-coupling reaction



1. Introduction

Many nematic and smectic molecules for liquid crystal displays (LCDs) are bi-phenyl or tri-phenyl compounds, e.g., homologues of 5CB [1–3]. However, liquid crystalline

CONTACT Guang Hu  guanghu2019@hyit.edu.cn  Key Laboratory for Palygorskite Science and Applied Technology of Jiangsu Province, National & Local Joint Engineering Research Center for Mineral Salt Deep Utilization, Faculty of Chemical Engineering, Huaiyin Institute of Technology, Huaian, Jiangsu, 223003, P. R. China; Department of Chemistry, Faculty of Science and Engineering, University of Hull, Cottingham Road, Kingston Upon Hull, HU6 7RX, UK.

materials with higher degree of aromatic conjugation have been proposed in recent years as novel organic semiconductors in plastic electronics [4–16]. Particularly, the least ordered nematic liquid crystalline materials with intrinsically low viscosity are preferred to form high-quality thin layers or films with a low concentration of charge traps in opto-electronic devices [17, 18].

Highly conjugated, fused, aromatic carbazoles have attracted much attention to construct organic semiconductor compounds due to strong luminescence, reversible oxidation processes, good hole-transporting capability, high chemical/environmental stability, and ease of functionalization [8]. Furthermore, the design of alkyl chains attached to carbazole moieties in lateral or terminal positions could also improve material solubility, lessen molecular aggregation, and adjust transition temperatures. The hetero-atoms, such as N, S, or O, in aromatic backbones to construct organic semiconductors have also been of great interest in materials chemistry due to the improved opto-electronic properties [19–23]. Therefore, in this work, novel alkyl-substituted (bisthiophene)benzene carbazole liquid crystals were designed and synthesized to study their mesomorphic behavior, transition temperatures, and physical properties. The influence of the length of alkyl chains in the symmetrical terminal positions of carbazoles units on the exhibition of liquid crystalline mesophases was also investigated and discussed in this paper.

2. Experimental

2.1. Materials and methods

All commercially available starting materials and reaction intermediates, reagents, and solvents were obtained from British Aldrich, Strem Chem. Inc., Acros, or Lancaster Synthesis and were used as supplied, unless otherwise stated. ^1H and ^{13}C NMR spectra were recorded using a Japanese JEOL Lambda 400 spectrometer with an internal standard of tetramethylsilane (TMS). Infrared (IR) spectra were recorded using an American PerkinElmer Paragon 1000 Fourier Transform-Infrared (FT-IR) spectrometer. Mass spectra were performed using American Quadrupole MS PerkinElmer gas chromatography/mass spectrometer (GC/MS) or Maldi-MS Bruker 384 spot anchorchip. The melting point and transition temperatures for each final compound were measured using polarizing optical microscopy (POM), with a Mettler FP-5 hot-stage and an American Olympus BH2 polarizing microscope. UV-Visible absorbance spectra were measured using a American Thermo Scientific Evolution 220 UV-Visible Spectrometer. The ionization potential (IP) of the compounds was measured electrochemically by cyclic voltammetry using a computer-controlled scanning potentiostat (British Solartron 1285), which functions as wave generator, potentiostat, and current-to-voltage converter. The Corrware and Corrview software packages were used to control and record the cyclic voltammetry experiments, respectively. The electron affinity (EA) was estimated by subtraction of the optical band edge (E_g), taken as the energy of the onset of absorption of the compound from the IP. Although this approximation does not include a correction for the exciton binding energy, the values obtained agree within ± 0.05 eV with those measured electrochemically in our laboratory for other classes of reactive mesogen [9].

2.2. Material synthesis

2.2.1. 1,4-Bis-(thien-2-yl)benzene (3)

A mixture of $\text{Pd}(\text{PPh}_3)_4$ (0.60 g, 0.52 mmol), 1,4-dibromobenzene (1) (6.00 g, 25.43 mmol), 2-thienylboronic acid (2) (10.00 g, 76.29 mmol), K_2CO_3 (14.05 g, 101.72 mmol), H_2O (50 cm^3), and DME (100 cm^3) was heated at reflux overnight. The cooled reaction mixture was poured into H_2O (150 cm^3) and the crude product isolated by filtration under reduced pressure. The crude product was stirred with methanol for 3 h, and the residual solid isolated by filtration under reduced pressure to afford the desired product as a pale-yellow solid (5.99 g, 97%).

Melting Point/ $^\circ\text{C}$: 208 (Lit. 204-206) [24].

^1H NMR (CDCl_3) δ_{H} : 7.63 (4H, d, $J = 1.0$ Hz), 7.35 (2H, dd, $J = 7.2$ & 1.0 Hz), 7.31 (2H, dd, $J = 5.2$ & 1.0 Hz), 7.11 (2H, dd, $J = 4.0$ & 1.6 Hz).

MS m/z (EI): 244, 243, 242 (M^+ , M100).

2.2.2. 1,4-Bis-(5-Bromothiophen-2-yl)benzene (4)

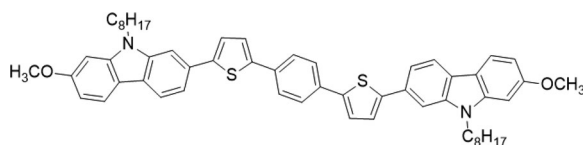
N-bromosuccinimide (NBS) (0.84 g, 4.72 mmol) was added in a small portion into a solution of 1,4-bis-(thien-2-yl)benzene(3) (0.54 g, 2.28 mmol) in DMF (20 cm^3) in the dark. The resultant mixture was stirred overnight at room temperature. The reaction mixture was diluted with ethanol (50 cm^3) and stirred for 1 h. A pale-yellow precipitate was filtered off, washed with ethanol ($3 \times 50 \text{ cm}^3$), and dried under reduced pressure to give the desired product (0.81 g, 94%).

Melting Point/ $^\circ\text{C}$: 255(Lit. 251-252) [24].

^1H NMR (CDCl_3) δ_{H} : 7.51 (4H, d, $J = 1.0$ Hz), 7.08 (2H, d, $J = 4.0$ Hz), 7.04 (2H, d, $J = 4.0$ Hz).

MS m/z (EI): 402, 401, 400(M^+).

2.2.3. 1,4-Bis-[5-(7-Methoxy-9-octyl-carbazol-2-yl)thiophen-2-yl]benzene (A)



A mixture of 1,4-bis-(5-bromothiophen-2-yl)benzene (4) (0.20 g, 0.50 mmol), $\text{Pd}(\text{OAc})_2$ (0.01 g, 0.045 mmol), K_2CO_3 (0.42 g, 3.00 mmol), (7-methoxy-9-octyl-carbazole-2-yl)boronic acid (5) (0.53 g, 1.50 mmol), and H_2O (2 cm^3) in DME (20 cm^3) was heated at reflux overnight. Then, the cooled reaction mixture was washed with water (100 cm^3) and extracted with DCM ($3 \times 100 \text{ cm}^3$). The combined organic layers were washed with water ($2 \times 100 \text{ cm}^3$), dried (MgSO_4), filtered, and then concentrated down under reduced pressure. The residue was purified using column chromatography [silica, DCM/hexane 5:10] to afford the desired product as a yellow solid (0.32 g, 76%).

Melting Point/ $^\circ\text{C}$: Cr 263 N 266 I.

^1H NMR (CDCl_3) δ_{H} : 7.99 (2H, d, $J = 8.0$ Hz), 7.96 (2H, d, $J = 8.8$ Hz), 7.69 (4H, d, $J = 0.8$ Hz), 7.57 (2H, d, $J = 0.8$ Hz), 7.52 (2H, dd, $J = 8.0$ & 1.6 Hz), 7.39 (2H, d,

$J = 4.0$ Hz), 7.38 (2H, d, $J = 3.6$ Hz), 6.86 (4H, dd, $J = 6.8$ & 2.0 Hz), 4.30 (4H, t, $J = 7.6$ Hz), 3.95 (6H, s), 1.90 (4H, quint, $J = 7.2$ Hz), 1.26-1.46 (20H, m), 0.88 (6H, t, $J = 6.8$ Hz).

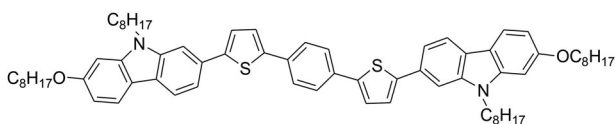
^{13}C NMR (CDCl_3): 159, 145, 143, 141, 134, 130, 125, 124, 121, 117, 107, 105, 94, 56, 43, 32, 29, 28, 27, 23, 14.

IR $\nu_{\text{max}}/\text{cm}^{-1}$: 2921, 2850, 1600, 1508, 1483, 1458, 1351, 1253, 1166, 1148, 1060, 1033, 951, 834, 790, 769.

MS m/z (MALDI): 859, 858, 857 (M^+ , M100).

Combustion analysis: Expected: C, 78.46%; H, 7.05%; N, 3.27%; S, 7.48%; Obtained: C, 78.44%; H, 7.05%; N, 3.36%; S, 7.67%.

2.2.4. 1,4-Bis-{5-[9-octyl-7-(octyloxy)-carbazol-2-yl]thiophen-2-yl}benzene (B)



A mixture of $\text{Pd}(\text{PPh}_3)_4$ (0.01 g, 0.008 mmol), 1,4-bis-(5-bromothiophen-2-yl)benzene (**4**) (0.20 g, 0.50 mmol), [N-octyl-7-(octyloxy)-carbazol-2-yl]boronic acid (**6**) (0.68 g, 1.5 mmol), K_2CO_3 (0.42 g, 3.00 mmol), and H_2O (2 cm^3) in DMF (30 cm^3) was heated at 80°C overnight. The cooled reaction mixture was washed with water (100 cm^3) and extracted with DCM ($3 \times 100\text{ cm}^3$). The combined organic layers were washed with water ($2 \times 100\text{ cm}^3$), dried (MgSO_4), filtered, and then concentrated under reduced pressure. The residue was purified using column chromatography [silica, DCM/hexane 5:10] to afford the desired product as a yellow solid (0.38 g, 73%).

Melting Point/ $^\circ\text{C}$: 248.

^1H NMR (CDCl_3) δ_{H} : 7.98 (2H, d, $J = 8.0$ Hz), 7.94 (2H, d, $J = 8.4$ Hz), 7.69 (4H, s), 7.56 (2H, s), 7.51 (2H, d, $J = 8.0$ Hz), 7.39 (4H, dd, $J = 6.4$ & 2.4 Hz), 6.85 (4H, dd, $J = 7.2$ & 2.0 Hz), 4.28 (4H, t, $J = 7.2$ Hz), 4.10 (4H, t, $J = 6.8$ Hz), 1.91 (8H, m), 1.26-1.53 (40H, m), 0.90 (6H, t, $J = 7.2$ Hz), 0.87 (6H, t, $J = 7.2$ Hz).

^{13}C NMR (CDCl_3): 159, 145, 142, 141, 134, 130, 126, 124, 121, 117, 108, 105, 94, 68, 44, 32, 29, 26, 22, 14.

IR $\nu_{\text{max}}/\text{cm}^{-1}$: 2921, 2850, 1599, 1483, 1460, 1356, 1254, 1166, 1146, 1063, 1029, 949, 834, 823, 791, 769.

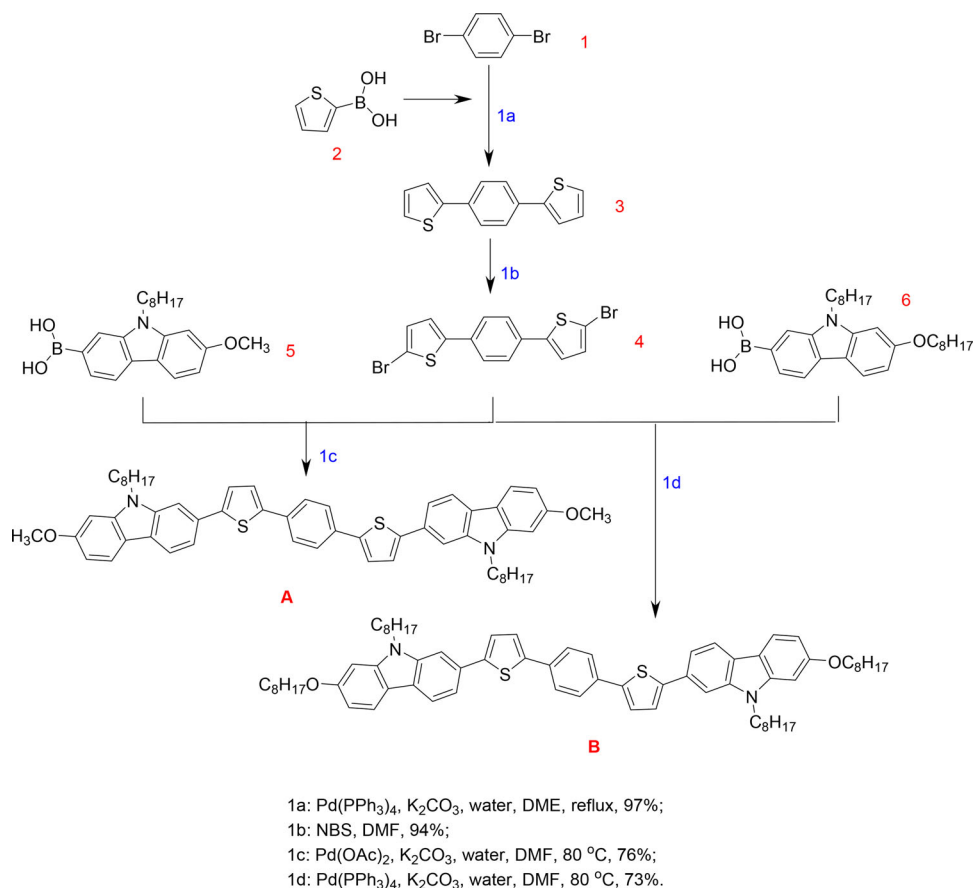
MS m/z (MALDI): 1055, 1054, 1053 (M^+ , M100).

Combustion analysis: Expected: C, 79.80%; H, 8.42%; N, 2.66%; S, 6.09%; Obtained: C, 79.77%; H, 8.47%; N, 2.61%; S, 6.15%.

3. Results and discussion

3.1. Synthetic discussion

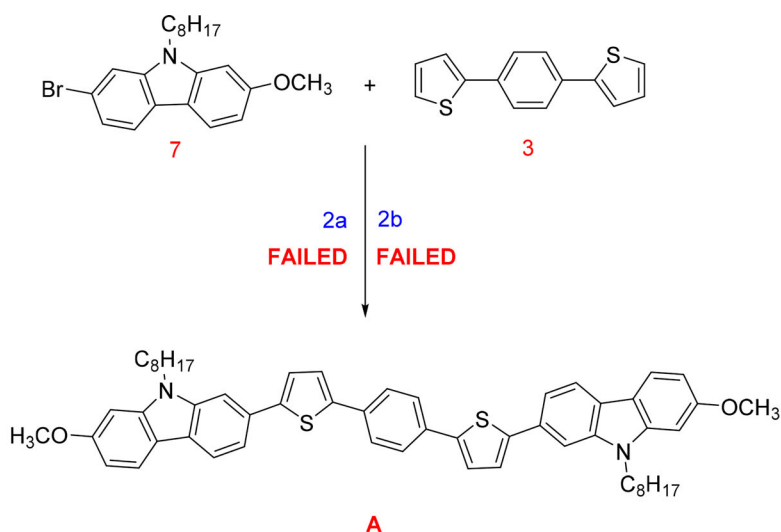
The two structural isomers **A** and **B** were synthesized as shown in the reaction Scheme 1. A Suzuki aryl-aryl, cross-coupling reaction was carried out to give 1,4-bis-(thien-2-yl)benzene(**3**) in excellent yield (97%). A possible reason for high yield is that



Scheme 1. The reaction pathway used to synthesize the (bisthiophene)benzene carbazole **A** and **B**

work-up of the reaction system is relatively simple, involving just washing away the impurities with methanol due to the relative insolubility of compound **3**. The compound **3** was then brominated by using NBS in DMF in darkness to give 1,4-*bis*-(5-bromothiophen-2-yl)benzene (**4**) in excellent yield (94%). The syntheses of the boronic acids **5** and **6** in Schemes 1 have been reported in our previous papers [8, 9], but used for synthesizing different final products in this paper. The boronic acid **5** was reacted with the dibrominated aromatic core **4** in a Suzuki aryl-aryl cross-coupling reaction using $\text{Pd}(\text{OAc})_2$ as catalyst, K_2CO_3 aqueous as base and DMF as solvent to give 1,4-*bis*-[5-(7-Methoxy-9-octyl-carbazol-2-yl)thiophen-2-yl]benzene (**A**) with good yield 76%. 1,4-*bis*-{5-[9-octyl-7-(octyloxy)-carbazol-2-yl]thiophen-2-yl}benzene (**B**) (73%) was synthesized under a similar Suzuki aryl-aryl cross-coupling reaction condition between compounds **4** and **6** catalyzed by $\text{Pd}(\text{PPh}_3)_4$ using aqueous K_2CO_3 and DMF as solvent.

Aryl carbon-carbon (C-C) single bond formation is of vital importance in synthetic organic chemistry. Generally, this process can be achieved with one arene functionalized with a halogen atom, e.g., bromine or iodine, reacting with the other arene containing organometallic moiety, e.g., $-\text{B}(\text{OH})_3$, $-\text{Sn}(\text{Bu})_3$, $-\text{Mg}$, which are representative of Suzuki Coupling [25, 26], Stille Coupling [27, 28], and Grignard reaction [29, 30], respectively. Sometimes direct arylation through C-H bond activation and cleavage is favored to



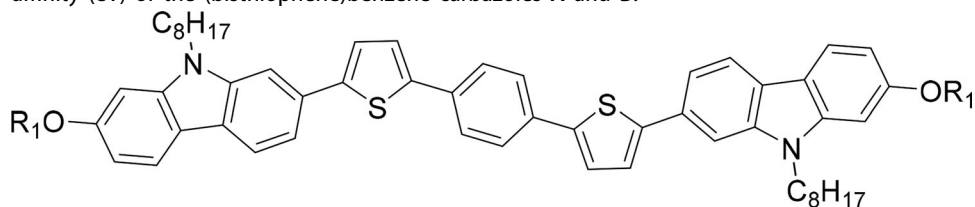
2a. K_2CO_3 (3 eq.), Pivalic acid (0.5 eq.), $\text{Pd}(\text{OAc})_2$ (0.05 eq.), PCy_3HBF_4 (0.2 eq.), DMF, 100 °C.

2b. K_2CO_3 (3 eq.), Pivalic acid (0.5 eq.), $\text{Pd}(\text{OAc})_2$ (0.05 eq.), PCy_3HBF_4 (0.2 eq.), NMP, 100 °C.

Scheme 2. Failed direct arylation pathway for synthesizing compound A

form aryl C-C bonds, due to a reduction in the number of synthetic steps required to achieve the same conversion [31, 32]. However, the direct arylation method is not always effective for aryl C-C bond formation. For instance, the direct arylation reaction, to create compound A between compounds 7 and 8 using DMF or NMP as solvent, was unsuccessful as shown in Scheme 2. In theory, thiophene moieties are excellent substrates for direct arylation reactions, due to the typically facile palladation through a concerted metalation-deprotonation (CMD) pathway, which renders the reaction highly selective for the 2- or 5-positions of the thiophene moieties [33]. Therefore, compounds 7 and 8 should be ideal as starting materials for direct arylation reactions. In this work, this reaction failed. According to the CMD mechanism of direct arylation [34, 35], the reaction steps include the oxidative addition of palladium to the C-Br bond of an aryl bromide, the exchange of the halogen ligand, deprotonation of the thiophene substrate with simultaneous formation of a metal-carbon bond, and then, the formation of an important transition state that determines whether the direct arylation can be achieved or not, and reductive elimination of the transition state. The energy required to form the transition state can be divided into two components including the energy of distorting the C-H bond of thiophene moiety and the interaction energy between distorted fragment and palladium center, according to density functional theory (DFT) calculations of the CMD mechanism [35, 36]. The bromo-substituted carbazole-derivate 7 is sterically bulky and may, therefore, require more energy to form a palladium active center to react with the distorted C-H bond of thiophene moiety. Furthermore, the bulky structure of the bromo-substituted carbazole-derivate is more likely to trap the palladium center, preventing the closing of distorted C-H bond. Therefore, as direct arylation was not possible, compound 7 was first lithiated, quenched with a boronate ester, and then hydrolyzed to obtain the corresponding carbazole-derivate boronic acid 5. Compound 3 was brominated in the required positions to obtain the compound 4.

Table 1. The phase transition temperatures, ionization potential (eV), band gap (eV), and electron affinity (eV) of the (bisthiophene)benzene carbazoles **A** and **B**.



Compound	R ₁	Phase Transition Temperatures (°C)	IP	E _g	EA
A	CH ₃	Cr 263-N ^a -266 Iso	5.46	2.67	2.79
B	C ₈ H ₁₇	Cr 248 Iso	5.45	2.67	2.78

N^a: transient nematic phase, Cr: crystalline, Iso: Isotropic.

Finally, Suzuki aryl-aryl cross-coupling reactions were carried out to obtain compounds **A** and **B** with good yields as shown in the Scheme 1. Compared with specific requirements for C-H bond and C-Br bond of direct arylation, Suzuki aryl-aryl coupling reactions are more tolerant of other functional groups present on the reagents and are also more tolerant of the steric demands of the reactants.

3.2. Mesomorphic behavior, liquid crystalline transition temperatures, energy levels, and band gaps of two isomers **a** and **B**

2,5-Disubstituted thiophene and 1,4-disubstituted phenyl rings are often present in organic semiconductor structures due to their influence on light-emitting characteristics, good charge transport properties, and chemical/environmental stability by influencing the molecular orbital energy levels and extending the degree of π -conjugation [24, 37]. Two thiophene/phenylene-based carbazoles were synthesized with different length of terminal aliphatic chains (R₁ = CH₃ or C₈H₁₇) attached to the phenyl ring of the aromatic core. The liquid crystalline transition temperatures (°C) of the compound **A** are collated in Table 1. The alkoxy substituents in a terminal position (R₁O) were varied in order to study the effect of the alkoxy chains on the mesomorphic behavior of the two compounds and their liquid crystalline transition temperatures. Of the (bisthiophene)-benzene carbazoles (**A** and **B**), only compound **A**, with the shorter alkoxy chains, possesses transient nematic liquid crystalline behavior (Cr 263-N^a-266 Iso). On increasing the length of alkoxy chains, the compound **B** was found to exhibit no observable liquid crystalline phases.

The insertion of linear and co-axial six-membered 1,4-disubstituted-phenyl ring into two nonlinear and non-co-axial five-membered 2,5-disubstituted thiophene rings strengthens the rigid structures of the aromatic main chain. It is a possible reason why compound **A** exhibits liquid crystalline mesomorphic behavior. However, the addition of phenylene at the central position of the aromatic main chain leads to a small angle between symmetrical sides of the aromatic backbone. Therefore, when the length of symmetrical terminal alkyl chains was increased, the nonlinear and non-co-axial structure of the whole molecule caused by the angle was strengthened. It can be well illustrated in Figure 1 by the optimized 3D geometry models using Chem3D/MM2 energy-minimized calculation. It could be further proved that the octyl-bithiophene-carbazole

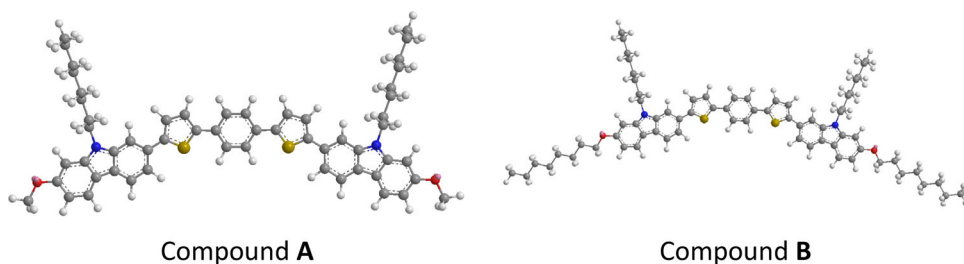


Figure 1. Optimized 3D geometry models using Chem3D/MM2 energy minimized calculation.

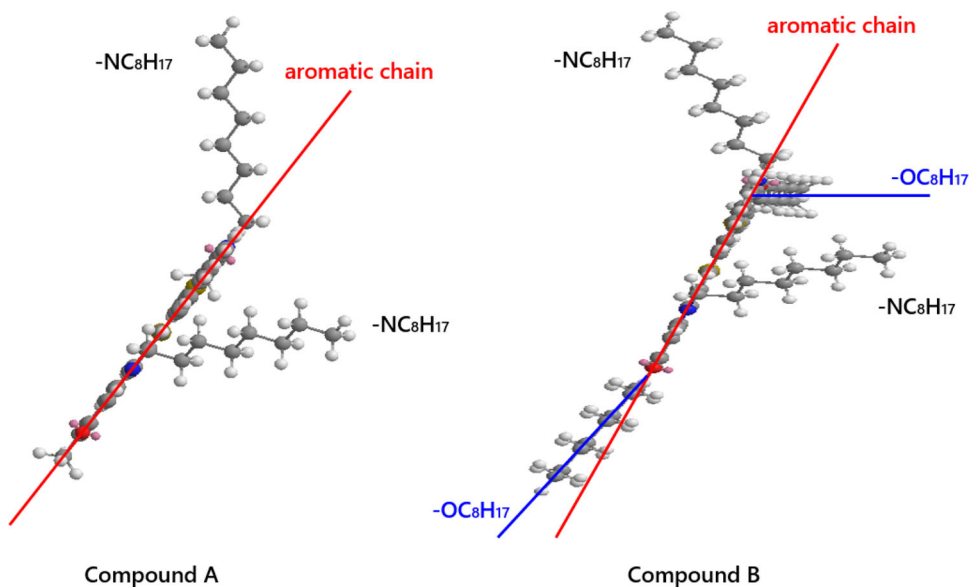


Figure 2. The 3D modeling contrast of a side perspective for compounds A and B.

molecule with only removing the phenylene from compound **B** shows nematic mesophase, which has been reported by our group before [9]. In addition, the two bonds of an oxygen atom attached to aromatic rings and alkyl chains also have an angle, which means the longer terminal alkyl chains further weaken the linear structure of aromatic main chains and thus decrease the length-to-breadth ratio of a whole molecule. The 3D modeling contrast of a side perspective for compounds **A** and **B** is shown in [Figure 2](#) to clearly reveal the unfavorable angle between the terminal octyl chains of compound **B** and the aromatic backbone. Therefore, it can be rationally explained why compound **A** is liquid crystalline while compound **B** is not.

The presence of additional 1,4-disubstituted phenyl rings not only affects the mesomorphic behavior, but also increases the liquid crystalline transition temperatures. It can be seen from [Table 1](#), that the melting point of the (bisthiophene)benzene carbazole **A** is significantly high due to an extended aromatic molecular core. The characteristic nematic droplets for compound **A** was observed on heating the sample into 265 °C using POM, shown in [Figure 3a](#). However, the another characteristic point singularities

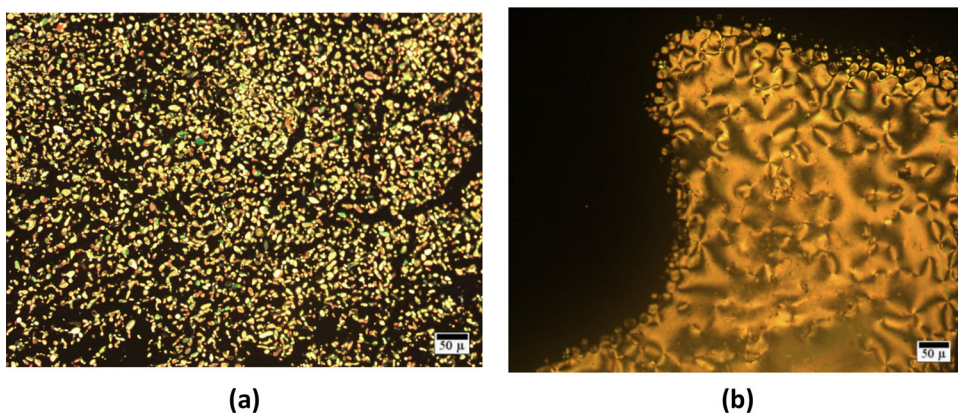


Figure 3. Characteristic nematic droplets and Schlieren texture observed for compound **A** on heating from room temperature to 265°C (a) and on cooling from the isotropic state to 266°C (b).

with four- and two-point brushes of a nematic mesophase were observed appropriately near the clearing point 266 °C only on cooling down from the isotropic state, see [Figure 3b](#), and disappeared at 263 °C. The compound **B**, containing longer alkyl chains than compounds **A**, exhibits lower melting points (Cr 248 °C-Iso). The presence of flexible alkyl chains usually serves to lower the intermolecular forces of attraction, e.g., Van der Waals forces, by increasing the intermolecular distance so that lower melting points and other liquid crystalline transition temperatures can be realized.

The cyclic voltammetry scanning curves of compounds **A** and **B** are shown in [Figure 4](#). Equation (1) was used to calculate the ionization potential (IP), as follows:

$$\text{IP (eV)} = E_{\text{ex}} - E_{1/2}^{\text{Fc}} + 0.425 + 4.7 \quad (1)$$

where E_{ex} is the onset voltage of the semiconductor compound peak, and $E_{1/2}^{\text{Fc}}$ is the average voltage derived from the peaks of oxidation and reduction $[(\text{Max} + \text{Min})/2]$ of the calibration sample of ferrocene. The constant 0.425 eV is that for the ferrocene standard and 4.7 eV is for the oxidation level of the silver-silver chloride electrode [38]. Thus, the ionization potential (IP) of compounds **A** and **B** is calculated as 5.46 eV and 5.45 eV, respectively.

[Figures 5](#) shows the UV-Vis absorption curves of compounds **A** and **B**. [Equation \(2\)](#) was used to calculate the energy gap (Eg) of the HOMO and LUMO energy levels, as follows:

$$\text{Eg (eV)} = hc/\lambda = 1240/\lambda(\lambda : \text{nm}) \quad (2)$$

where h is the Planck constant (4.135×10^{-15} eV s), c is the speed of light (3.0×10^{17} nm/s), $hc = 1240$ eV nm, and λ is the absorption maximum (nm) extracted from the UV-Vis absorption spectrum of the compound being investigated [38]. Therefore, as shown in [Figure 5](#) for compounds **A** and **B**, $\lambda = 463.45$ nm and $\lambda = 463.91$ nm, the band gaps, Eg, of compounds **A** and **B** can be calculated as both 2.67 eV approximately. The LUMO energy level (EA) was estimated by the subtraction of the value of the optical band gap (Eg) from the ionization potential (IP), which does not include any correction for the exciton binding energy.

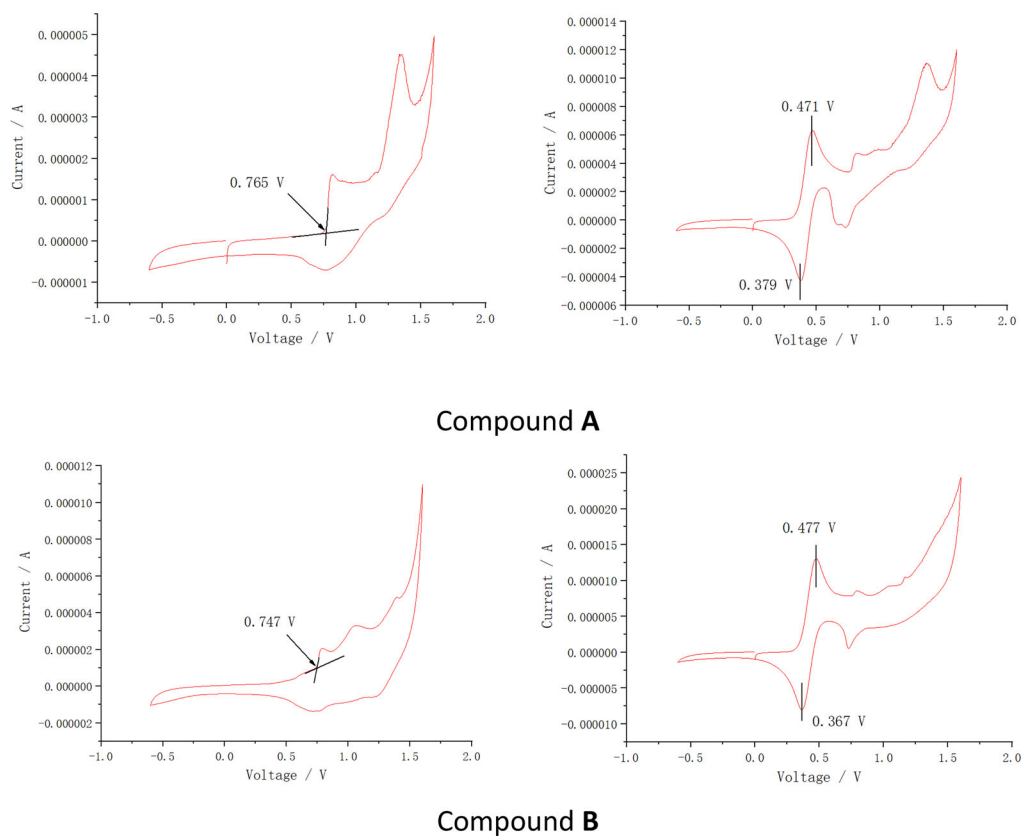


Figure 4. The cyclic voltammetry scanning curves of compounds **A** and **B**.

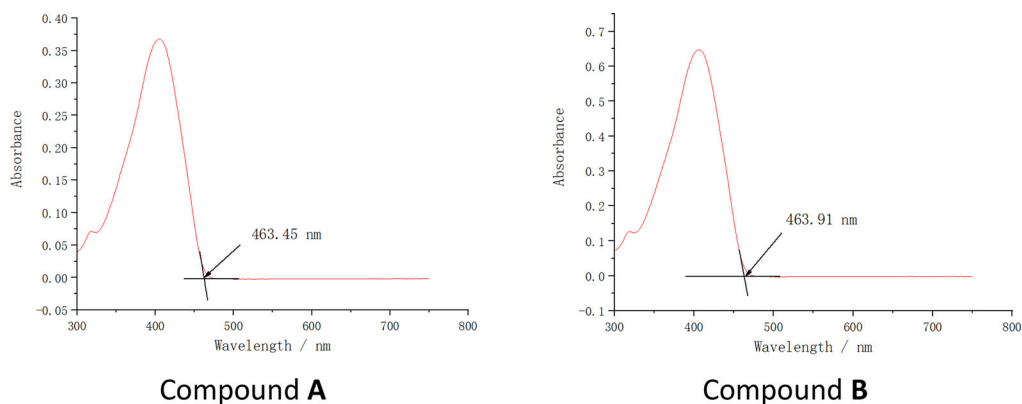


Figure 5. The UV-Vis absorption curves of compounds **A** and **B**.

The values for the ionization potentials (IP), energy gaps (E_g), and electron affinity (EA) of compounds **A** and **B** are collated in [Table 1](#), and they do not appear to be significantly influenced by the length of alkyl chains. The result is consistent with their electron density distribution of the HOMO and LUMO states mainly localized on the

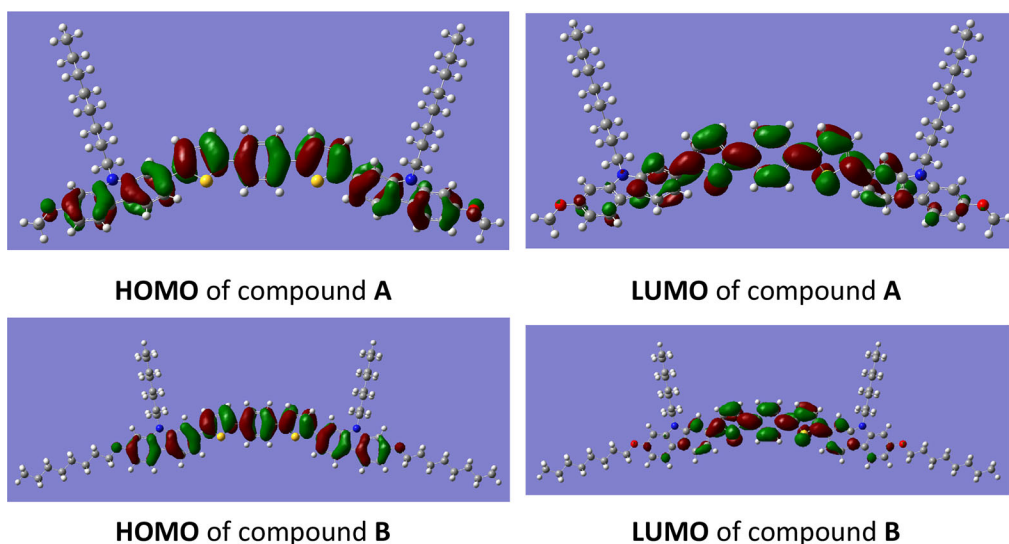


Figure 6. Electron density distribution of compounds **A** and **B** in the HOMO and LUMO states calculated by TD-DFT using Gaussian 09 at the B3PW91/6-31G (d) level.

sequentially aromatic units as predicted by TD-DFT using Gaussian09 at the B3PW91/6-31G (d) level, see [Figure 6](#).

Conclusions

Two structural isomers of (bisthiophene)benzene carbazoles **A** and **B** with different length of alkyl chains in symmetrical terminal positions were synthesized using optimized reaction pathways and exhibited different mesomorphic behavior but similar values of energy levels and band gaps. Only the isomer **A** with shorter terminal alkyl chains exhibits transient nematic liquid crystalline mesophases (Cr 263 °C -N^a-266 °C Iso). The longer octyl terminal chains of the isomer **B** in turn result in the strengthening of both kinds of small angles between symmetrical aromatic backbones and between terminal alkyl chains and the aromatic backbone. Simulated HOMO and LUMO states proved similar electron density distribution which mainly localized on the sequentially aromatic units.

Disclosure statement

No potential conflict of interest was reported by the authors.

Funding

National & Local Joint Engineering Research Center for Mineral Salt Deep Utilization, Huaiyin Institute of Technology [Grant Number: SF202010]; Huaiyin Institute of Technology [Grant Number: Z301B19582]; Science and Technology Foundation of Huai'an City [Grant Number: HAB202064]; University of Hull; China Scholarship Council.

References

- [1] G. Gray, K. J. Harrison, and J. A. Nash, *Electron. Lett.* **9** (6), 130 (1973). doi:10.1049/el:19730096
- [2] M. Hird, K. J. Toyne, and G. W. Gray, *Mol. Cryst. Liq. Cryst.* **206** (1), 187 (1991). doi:10.1080/00268949108037730
- [3] S. P. Kitney *et al.*, *Liq. Cryst.* **38** (8), 1027 (2011). doi:10.1080/02678292.2011.593198
- [4] S. M. Kelly, *Flat Panel Displays: Advanced Organic Materials* (The Royal Society of Chemistry, Cambridge, UK, 2000).
- [5] M. C. Yang, J. I. Hanna, and H. Iino, *J. Mater. Chem. C* **7** (42), 13192 (2019). doi:10.1039/C9TC03990B
- [6] C. M. Keum *et al.*, *Sci. Rep.* **8** (1), 699 (2018). doi:10.1038/s41598-018-19157-9
- [7] M. J. Han *et al.*, *ACS Cent Sci.* **4** (11), 1495 (2018). doi:10.1021/acscentsci.8b00465
- [8] G. Hu *et al.*, *Liq. Cryst.* **45** (7), 965 (2018). doi:10.1080/02678292.2017.1404156
- [9] G. Hu *et al.*, *Liq. Cryst.* **44** (11), 1632 (2017). doi:10.1080/02678292.2017.1306633
- [10] M. Ozaki *et al.*, *Liq. Cryst.* **45** (13–15), 2376 (2018). doi:10.1080/02678292.2018.1530375
- [11] Y. F. Wang, H. Iino, and J. I. Hanna, *Soft Matter*. **13** (37), 6499 (2017). doi:10.1039/c7sm01303e
- [12] S. Paul *et al.*, *J. Appl. Phys.* **118** (13), 135702 (2015). doi:10.1063/1.4931913
- [13] H. Iino and J. I. Hanna, *Polym. J.* **49** (1), 23 (2017). doi:10.1038/pj.2016.101
- [14] H. Monobe *et al.*, *Mol. Cryst. Liq. Cryst.* **647** (1), 119 (2017). doi:10.1080/15421406.2017.1289443
- [15] E. B. Melo *et al.*, *Mol. Cryst. Liq. Cryst.* **657** (1), 81 (2017). doi:10.1080/15421406.2017.1403232
- [16] K. Ohta *et al.*, *Mol. Cryst. Liq. Cryst.* **397** (1), 25 (2003). doi:10.1080/714965592
- [17] M. O'Neill and S. M. Kelly, *Adv. Mater.* **23** (5), 566 (2011). doi:10.1002/adma.201002884
- [18] R. J. Bushby, M. O'Neill, and S. M. Kelly, *Liquid Crystalline Semiconductors: materials, Properties and Applications* (Springer, Dordrecht, Netherlands, 2013).
- [19] O. Ostroverkhova, *Chem. Rev.* **116** (22), 13279 (2016). doi:10.1021/acs.chemrev.6b00127
- [20] C. Zhang and X. Zhu, *Acc. Chem. Res.* **50** (6), 1342 (2017). doi:10.1021/acs.accounts.7b00050
- [21] A. Hlel *et al.*, *Comput. Condens. Matter*. **3**, 30 (2015). doi:10.1016/j.cocom.2015.02.001
- [22] G. Turkoglu, M. E. Cinar, and T. Ozturk, in *Sulfur Chemistry*, Chapter 3, edited by X. Jiang (Springer Nature Switzerland AG, Basel, Switzerland, 2019), pp. 79–124.
- [23] H. Sahu *et al.*, *Phys. Chem. Chem. Phys.* **17** (32), 20647 (2015). doi:10.1039/c5cp02872h
- [24] A. Pelter, I. Jenkins, and D. E. Jones, *Tetrahedron* **53** (30), 10357 (1997). doi:10.1016/S0040-4020(97)00629-7
- [25] J. H. Kirchhoff *et al.*, *J. Am. Chem. Soc.* **124** (46), 13662 (2002). doi:10.1021/ja0283899
- [26] N. R. Lee *et al.*, *Org. Lett.* **20** (10), 2902 (2018). doi:10.1021/acs.orglett.8b00961
- [27] S. P. H. Mee, V. Lee, and J. E. Baldwin, *Angew. Chem. Int. Ed. Engl.* **43** (9), 1132 (2004). doi:10.1002/anie.200352979
- [28] J. H. Li *et al.*, *J. Org. Chem.* **70** (7), 2832 (2005). doi:10.1021/jo048066q
- [29] H. Zong *et al.*, *J. Org. Chem.* **77** (10), 4645 (2012). doi:10.1021/jo3004277
- [30] T. E. Hurst *et al.*, *Org. Lett.* **21** (11), 3882 (2019). doi:10.1021/acs.orglett.9b00773
- [31] H. Bohra and M. Wang, *J. Mater. Chem. A* **5** (23), 11550 (2017). doi:10.1039/C7TA00617A
- [32] C. Verrier *et al.*, *Beilstein J. Org. Chem.* **7**, 1584 (2011). doi:10.3762/bjoc.7.187
- [33] D. Schipper and K. Fagnou, *Chem. Mater.* **23** (6), 1594 (2011). doi:10.1021/cm103483q
- [34] S. I. Gorelsky, *Coord. Chem. Rev.* **257** (1), 153 (2013). doi:10.1016/j.ccr.2012.06.016
- [35] L. G. Mercier and M. Leclerc, *Acc. Chem. Res.* **46** (7), 1597 (2013). doi:10.1021/ar3003305
- [36] S. I. Gorelsky, D. Lapointe, and K. Fagnou, *J. Org. Chem.* **77** (1), 658 (2012). doi:10.1021/jo202342q
- [37] M. Mushrush *et al.*, *J. Am. Chem. Soc.* **125** (31), 9414 (2003). doi:10.1021/ja035143a
- [38] G. Hu *et al.*, *Phase Transit.* **93** (8), 759 (2020). doi:10.1080/01411594.2020.1775830